Food and Bioprocess Technology (2026) 19:314
https://doi.org/10.1007/s11947-026-04395-x

RESEARCH

Combined Effect of Ultrasound Pretreatment and Removal of Insoluble Solids on Fermentation with *Lactobacillus gasseri* and Pea Protein Rheology

Antonia Isabelly Monteiro do Anjos[1] · Shênia Santos Monteiro[2] · Anna Clara Batista de Sousa[1] · Marcus Vinícius Lia Fook[3] · Daniel Pens Gelain[2] · José Cláudio Fonseca Moreira[2] · Hugo Miguel Lisboa[1] · Matheus Augusto de Bittencourt Pasquali[1]

Received: 28 January 2026 / Accepted: 6 May 2026 / Published online: 14 May 2026
© The Author(s) 2026

Abstract

This study evaluated the synergistic effect of ultrasound pretreatment and insoluble solids removal on the fermentation of pea protein concentrate (*Pisum sativum* L.) by *Lactobacillus gasseri* and its implications for the kinetic, fermentative, and rheological properties of the system. Four experimental treatments were investigated: protein fermented by *L. gasseri* (P-LG), protein pretreated by ultrasound and fermented by *L. gasseri* (P-US-LG), soluble protein fermented by *L. gasseri* (S-LG), and soluble protein pretreated by ultrasound and fermented by *L. gasseri* (S-US-LG). The growth kinetics, based on total cell counts determined in a Neubauer chamber, was modeled using a modified Gompertz equation for the growth phase, whereas the post-peak phase was described only descriptively with an exponential decay function. Acidification was modeled using a four-parameter logistic equation. The rheological properties were evaluated using flow and oscillatory testing, with shear-sweep data fitted to the Ostwald-de Waele model. The results indicated that the removal of insoluble solids was associated with higher μ_{max} values and a shorter time to reach pH < 5.5, characterizing faster acidification in kinetic terms, while ultrasound modulated the microbial adaptation time in a manner dependent on the protein fraction. The non-centrifuged systems showed greater consistency and predominantly elastic viscoelastic behavior, while the soluble fractions exhibited lower viscosity and less organized structures. Radar visualization highlighted the distinct functional profiles among treatments. Taken together, the findings demonstrate that combined strategies of physical processing and lactic fermentation enable modulation of the techno functional properties of fermented plant proteins.

Keywords *Pisum sativum* L. · Probiotic · Viscosity · Fermentation kinetics

Introduction

The growing interest in plant-based proteins as sustainable alternatives to animal proteins reflects a global shift towards healthier and more environmentally responsible dietary patterns, driven by environmental, ethical, and public health concerns (Patil et al., 2025). Among them, pea protein stands out for its high-protein content (20–30% of the grain's dry weight), balanced amino acid profile with high levels of lysine, and low allergenicity (Lu et al., 2020; Taylor et al., 2021; Xu et al., 2023). However, technological limitations, such as low solubility, insoluble fractions, and the development of undesirable sensory attributes, still restrict its application in fermented and structured food systems (Farshi et al., 2024; Liu et al., 2022).

Previous studies demonstrate that ultrasound is a promising physical strategy for modifying pea proteins, promoting structural changes resulting from acoustic cavitation, such as particle size reduction and exposure of functional groups, leading to improvements in solubility, emulsification, and gelation (Barac et al., 2012; Patil et al., 2025;

✉ Shênia Santos Monteiro
shenia-monteiro@hotmail.com

[1] Federal University of Campina Grande, Academic Unit of Food Engineering, Campina Grande 58429-900, Brazil

[2] Department of Biochemistry, Federal University of Rio Grande Do Sul, Porto Alegre 90035-003, Brazil

[3] Federal University of Campina Grande, Academic Unit of Materials Engineering, Campina Grande 58429-900, Brazil

Shen et al., 2022). Independently, fermentation with lactic acid bacteria, especially *Lactobacillus* spp., has been extensively investigated in plant matrices, being associated with improved protein digestibility, the development of aromatic compounds, and the reduction of off-flavors, in addition to impacting microbial growth kinetics and the acidification of the medium (Erem and Kilic-Akyilmaz 2024; Kaleda et al., 2025; Zhang et al., 2025).

Despite advances in these technologies, a significant gap remains in the literature. Few studies have combined ultrasound and lactic fermentation in pea protein systems within the same experimental design. Furthermore, there is a lack of research that simultaneously evaluates microbial kinetics, acidification dynamics, and rheological behavior in fermented pea protein matrices, particularly regarding the impact of insoluble fractions.

Given this context, the hypothesis of this study is that ultrasound pretreatment, associated with the removal of insoluble solids, can promote structural modulation of pea protein that favors the adaptation and growth of *Lactobacillus gasseri*, accelerates acidification, and influences the rheological behavior of the fermented system. The distinguishing feature of this work is its integrated approach, which simultaneously evaluates growth kinetics, acidification parameters, and rheological properties, thereby providing a comprehensive assessment of the interactions between processing conditions and system responses. Thus, the objective of this study was to investigate the combined effects of ultrasound and insoluble solids removal on the fermentation of pea protein by *L. gasseri*, with the aim of developing sustainable functional ingredients with enhanced technological properties.

Materials and Methods

Materials

Pea protein concentrate (≥ 83% protein, 2% lipids, 0% carbohydrates, and 5% fiber) was obtained from Jhamal Natural (Brazil). The *Lactobacillus gasseri* strain (ATCC 33323) was obtained from the Tropical Cultures Collection–André Tosello Foundation (Campinas, Brazil). All reagents used were of analytical grade.

Preparation of the Culture and Fermentation Medium

Pea protein concentrate was dispersed in distilled water at a concentration of 160 mg/mL and homogenized manually to ensure uniform dispersion. The concentration of 160 mg/mL of pea protein concentrate was selected based on preliminary laboratory tests. This concentration maintained the system in a liquid state with suitable viscosity for homogeneous fermentation. It also provided sufficient protein substrate to support the growth of *L. gasseri* without excessive dilution of the medium. The suspension was then kept at 8 °C for 24 h to ensure complete hydration of the protein. After this period, the suspension was pasteurized at 80 °C for 30 min to reduce the naturally occurring microbial load (Akpabli-Tsigbe et al., 2023; Chen et al., 2024). It should be noted that this heat treatment can induce structural changes in proteins, with potential impacts on rheological properties; however, the same protocol was applied to all experimental groups, ensuring equivalent initial conditions for subsequent analyses.

A fraction of the pasteurized suspension was subjected to ultrasound pretreatment in an ultrasonic bath (ALTSONIC CLEAN 3PA, Ribeirão Preto-SP, Brazil), operating at 40 kHz and a nominal power of 100 W, for 10 min. This frequency was selected because it promotes stable cavitation and effective physical disruption in liquid food systems without causing excessive protein denaturation, while the nominal power ensures sufficient acoustic intensity for structural modification (Alrosan et al., 2026). The samples were placed in 500-mL glass reagent bottles containing 300 mL of the mixture, kept vertically, and fully submerged in the ultrasonic bath to ensure homogeneous exposure to the acoustic field. The total volume of water in the bath was kept below 30 °C by periodically replenishing it with ice, thereby minimizing thermal effects associated with the ultrasonic pretreatment. Ultrasound was applied prior to centrifugation as a pretreatment to increase protein solubilization in pea protein concentrate, with the aim of breaking down protein aggregates and promoting the release of soluble components from the original matrix, allowing the subsequent centrifugation step to separate the fractions according to the solubilization effects induced by ultrasound. Figure 1 presents a schematic representation of the experimental design and preparation steps of the four treatments applied to pea protein concentrate.

Samples not subjected to ultrasonic pretreatment were designated P (dispersed protein), while those subjected to pretreatment in an ultrasonic bath were designated P-US. A portion of these samples was centrifuged, resulting in samples S (soluble protein) and S-US (soluble protein pretreated in an ultrasonic bath).

After applying all pretreatments (ultrasound and/or centrifugation), the P, P-US, S, and S-US suspensions were inoculated with *L. gasseri* and subjected to fermentation. The fermented samples were named P-LG, P-US-LG, S-LG, and S-US-LG, respectively. In all treatments, inoculation was performed after the pretreatments.

The four experimental treatments were fermented with *L. gasseri* for 48 h at 37 °C. For this, *L. gasseri* was reactivated in MRS broth (KASVI, Brazil) for 48 h at 37 °C. The

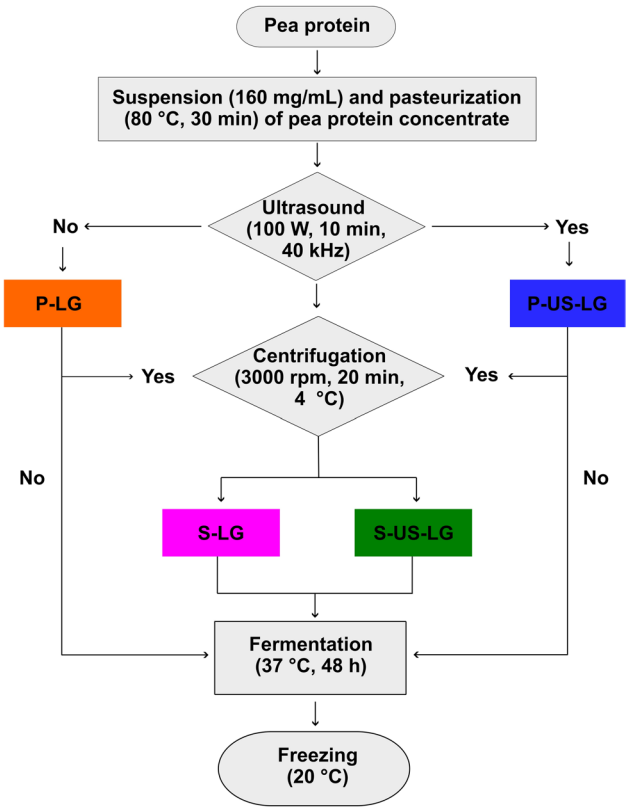


Fig. 1 Flowchart of the process for preparing the four treatments applied to pea protein concentrate. The pea protein concentrate was dispersed in water (160 mg/mL) and pasteurized (80 °C, 30 min), followed by optional pretreatment with ultrasound (100 W, 40 kHz, 10 min) and/or centrifugation (3000 rpm, 20 min, 4 °C) for the removal of insoluble solids. The resulting fractions were fermented with *L. gasseri* (37 °C, 48 h) and frozen (20 °C) to stop fermentation and subsequently analyzed for rheological properties. The experimental conditions were defined as P-LG (protein fermented with *L. gasseri*; orange), P-US-LG (protein pretreated with ultrasound and fermented with *L. gasseri*; blue), S-LG (soluble protein fermented with *L. gasseri*; pink), and S-US-LG (soluble protein pretreated with ultrasound and fermented with *L. gasseri*)

reactivated *L. gasseri* cells were separated by centrifugation (Refrigerated centrifuge NT 815, Novactenica, Brazil), equipped with a horizontal rotor, at 2000 rpm for 10 min. The supernatant was discarded, and the cell mass (pellet) was suspended in sterile distilled water (121 °C, 15 min), cooled to room temperature. The four treatments were inoculated with 6 Log cells/mL of *L. gasseri*. The samples were homogenized and incubated in partially threaded Falcon-type tubes to establish conditions of limited oxygen availability without agitation throughout the fermentation period. During the fermentation period, aliquots were removed for kinetic study. In the first 24 h, kinetic monitoring was performed at 2—h intervals, and subsequently at 40 and 48—h intervals. Cell counts were performed by direct counting in a Neubauer chamber, as well as the determination of pH and total soluble solids (°Brix). It should be noted that counting in a Neubauer chamber provides an estimate of the total number of cells; however, in protein-rich matrices, such as pea protein suspensions, dispersed particles and protein aggregates can interfere with visualization, potentially leading to overestimation or variability in cell counts. Such interference can affect the accuracy of calculated growth parameters, including the microorganism's adaptation time to the medium (λ) and the apparent maximum growth rate (μ_{max}). To minimize these effects, samples were properly diluted and homogenized before counting. Accordingly, changes observed after t_{peak} represent apparent post-peak changes in total counted cells and should not be interpreted as direct measurements of cell death or viability loss.

Modeling the Growth of *L. gasseri*

To model the growth kinetics of *L. gasseri* in the four experimental treatments, the data were segmented into two distinct phases: (i) adaptation phase and exponential growth (0 h—t_{peak}) and (ii) stationary and decline phase (t_{peak}—48 h). The t_{peak} time was defined by direct inspection of the growth curves, considering the time corresponding to the highest average cell concentration value observed during fermentation, calculated from the experimental replicates. The modified Gompertz model was fitted to the data corresponding to phase (i), whereas phase (ii) was explored with an exponential decay model with an asymptotic plateau only as a descriptive approximation of the apparent post-peak behavior.

Modified Gompertz Model

The lag (adaptation) phase and exponential growth of *L. gasseri* in the four experimental treatments obtained from pea protein concentrate were described using the modified Gompertz model (Eq. 1), which is widely used to represent the sigmoidal behavior of microbial growth.

$$Y(t) = y_0 + A \times exp(-exp((\mu_{max} \times 2.718/A) \times (\lambda - t) + 1)) \quad (1)$$

where $Y(t)$ is the cell concentration (Log cell/mL) at time t (h), y_0 is the initial cell concentration (Log cell/mL), A is the asymptotic increase in logarithmic units (with $y_0 + A$ approximating the maximum cell concentration), μ_{max} is apparent maximum growth rate (Log/h), and λ is the time of adaptation of the microorganism to the medium (h).

Exponential Decay Model

An exponential decay model with an asymptotic plateau (Eq. 2) was employed as a descriptive approximation of the

apparent post-peak decrease after the maximum counted cell concentration was reached.

$$Y(t) = y_{\infty} + (y_{peak} - y_{\infty}) \times exp(-k \times (t - t_{peak})) \quad (2)$$

where $Y(t)$ is the cell concentration (Log cell/mL) at time t (h) for $t \geq t_{peak}$, y_{peak} is the maximum cell concentration (Log cell/mL) observed at t_{peak}, y_{∞} is the asymptotic logarithm of the cell concentration during the cell decline phase, and k is the apparent decay rate constant.

Acidification Kinetics and Total Soluble Solids

The variation in pH throughout the fermentation of the different experimental treatments obtained from pea protein concentrate fermented with *L. gasseri* was described using a four-parameter logistic model (Eq. 3). This model was selected for its suitability in representing microbial acidification processes characterized by sigmoidal behavior, including an initial lag phase, followed by a sharp drop in pH and, subsequently, a stabilization phase.

$$pH(t) = A + B/(1 + exp(-(t - C)/D)) \quad (3)$$

where A represents the initial asymptotic pH, B corresponds to the total pH change (ΔpH), C refers to the time at which the maximum acidification rate occurs, and D is associated with the slope of the acidification curve, reflecting the rate of pH decrease.

The total soluble solids content was also determined over the fermentation period for all experimental treatments, in order to monitor the consumption of soluble substrates during the fermentation process.

Rheological Properties

The rheological properties of the four experimental treatments were evaluated at 25 °C and 37 °C, at the initial moment of fermentation with *L. gasseri* (0 h) and after 48 h of fermentation. For measurements, 2 mL of the sample was used in the measuring cell. The rheological properties were determined using a HAAKE MARS III rotational rheometer (Thermo Fisher Scientific), equipped with an MTMC temperature control system, using a titanium (P60 Ti) cone-plate geometry with an angle of 0.5° and a 0.500—mm gap. The samples were manually loaded into the center of the plate to avoid incorporating bubbles and allowed to stand for 0.5 min before measurements. The apparent viscosity and shear stress curves were obtained in controlled shear rate mode, applying a logarithmic ramp from 0.1 to 1000 s^{-1} for 2.5 min. Subsequently, the viscoelastic properties were evaluated by oscillatory frequency sweeps conducted under a constant strain of 1%, assumed to lie within the linear viscoelastic region, over the frequency range 0.1 to 100 Hz. The reduced test time and rigorous temperature control minimized evaporation effects during the analyses.

The Ostwald-de Waele model was fitted to the experimental viscosity data as a function of shear rate (Eq. 4).

$$\eta = k \times \gamma^{n-1} \quad (4)$$

where η is the apparent shear viscosity (Pa·s), γ is the shear rate (s^{-1}), k is the consistency index (Pa·s^n), and n is the flow behavior index.

Statistical Analysis

All experiments were performed in triplicate ($n = 3$) or quintuplicate ($n = 5$), as specified, and the data are presented as means ± standard deviation. The statistical differences between the groups were assessed using analysis of variance (ANOVA), followed by Tukey's post-hoc test for multiple comparisons, considering a significance level of $p < 0.05$.

The kinetic growth parameters of *L. gasseri* were estimated by nonlinear regression using GraphPad Prism software, version 10.0 (GraphPad Software, San Diego, CA, USA). The equations used were customized based on the behavior observed in the experimental data, to ensure the best representation of the different phases of *L. gasseri* growth kinetics in the experimental treatments obtained from pea protein concentrate.

The acidification kinetics and rheological parameters were estimated by nonlinear regression using the Levenberg–Marquardt method. The fitting was performed using Statistica software, version 7.0 (StatSoft Inc., Tulsa, OK, USA). The quality of fit of the models (modified Gompertz, exponential decay, four-parameter logistic model, and Ostwald-de-Waele) was evaluated using the coefficient of determination (R^2). For models showing inadequate fit, parameter estimates were treated only descriptively and were not subjected to inferential statistical comparison.

To provide an integrated visual summary of the fermentative and rheological responses after 48 h of fermentation at 37 °C, a radar plot (spider plot) was constructed using normalized values of selected key parameters: apparent maximum growth rate (μ_{max}), pH at the end of fermentation (pH), variation in total soluble solids (Δ°Brix), consistency index (k), and flow behavior index (n). The values were normalized per variable using the min–max scale (0 to 1) to allow direct comparison between treatments. The radar plot was generated in R (version 4.3.1; R Core Team, 2023) with the tidyverse and fmsb packages (or ggplot2 with coord_polar) and is presented as a descriptive visualization tool that complements the results of the univariate and factorial ANOVA.

Results

Influence of Ultrasound Pretreatment and Removal of Insoluble Solids on the Growth Kinetics of *L. gasseri*

The growth curves of *L. gasseri* in the four experimental treatments are shown in Fig. 2. In all treatments, a typical kinetic profile was observed, with an initial phase of exponential growth up to t_{peak} (the time at which maximum cell growth was observed), followed by a phase of cell decline. The experimental data (mean ± standard deviation; $n = 5$) were adequately described by the modified Gompertz model during the growth phase. In contrast, the exponential decay model showed limited adequacy for the post-peak phase and was used only as a descriptive approximation.

In the P-LG treatment (Fig. 2A), the number of cells increased rapidly in the first hours of fermentation, reaching an average value of 8.7 ± 0.223 Log cells/mL at 8 h, followed by a gradual decline, without showing a stationary phase over time. The P-US-LG treatment (Fig. 2B) showed

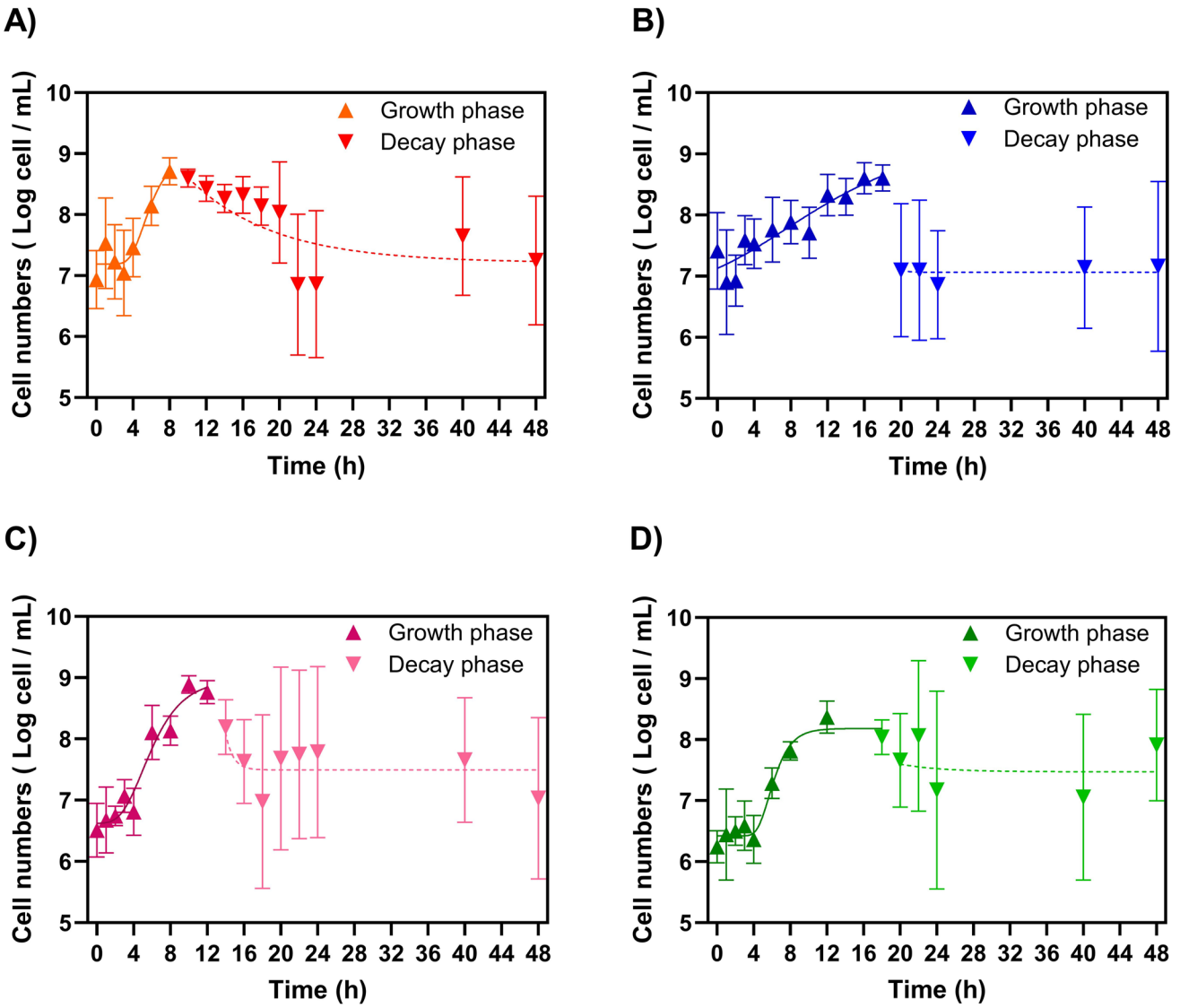


Fig. 2 Growth curves of *L. gasseri* for four experimental treatments applied to pea protein concentrates fermented by *L. gasseri*. The points represent the experimental means accompanied by the standard deviation ($n = 5$) of the total number of cells over the fermentation time for each treatment: **A** P-LG (protein fermented with *L. gasseri*; orange and red), **B** P-US-LG (protein pretreated with ultrasound and fermented with *L. gasseri*, blue), **C** S-LG (soluble protein fermented with *L. gasseri*; pink), and **D** S-US-LG (soluble protein pretreated with ultrasound and fermented with *L. gasseri*, green). Solid lines correspond to the adjustments of the Gompertz model applied to the growth phase up to the peak time (t_{peak}, maximum growth), whereas dashed lines represent descriptive exponential fits for the post-peak phase

progressive growth up to 18 h of fermentation, reaching a cell count of 8.6 ± 0.215 Log cells/mL, followed by a decline shortly after reaching t_{peak}, with a relatively stable cell count maintained until the end of fermentation.

For the S-LG treatment (Fig. 2C), a rapid increase in the number of cells was observed in the first hours of fermentation, reaching a maximum average value of 8.8 ± 0.190 Log cells/mL at 12 h, followed by a reduction in the number of cells in the following hours. The S-US-LG treatment (Fig. 2D) showed gradual growth up to 12 h, with a maximum average value of 8.4 ± 0.264 Log cells/mL, showing a slight reduction in the number of cells after reaching t_{peak}, but maintaining high values until the end of fermentation.

Table 1 summarizes the estimated parameters for the four experimental treatments with mean ± standard deviation, along with the corresponding coefficient of determination (R^2) for each adjustment. The coefficients of determination (R^2) ranged from 0.8644 to 0.9723 among the four experimental treatments, indicating a satisfactory to excellent fit of the modified Gompertz model to the experimental data. The S-US-LG treatment, in particular, showed the highest R^2 (0.9723), reflecting a very good agreement between the model predictions and the observed growth data. Furthermore, one-way ANOVA indicates that the four treatments (P-LG, P-US-LG, S-LG, and S-US-LG) produce statistically significant differences in initial concentration (y_0), apparent maximum growth rate (μ_{max}), and adaptation or latency phase (λ). In contrast, the overall increase in cell number (A) did not differ significantly between treatments. These results suggest that, although pretreatments (ultrasound and/or centrifugation) affect the apparent maximum growth rate and adaptation phase, they do not substantially alter the overall increase in cell number.

The initial cell count values estimated by the Gompertz model (y_0) differed between treatments ($p < 0.05$), ranging from 6.42 ± 0.12 to 7.19 ± 0.13 Log cells/mL, with P-LG showing the highest values and S-US-LG the lowest. Although inoculation was standardized to approximately 6 Log cells/mL in all treatments, the variation observed in the initial estimated values (y_0) can be attributed to methodological and biological factors inherent to counting in a Neubauer chamber and to the adjustment of the kinetic model. Additionally, y_0 corresponds to a parameter estimated by adjusting the modified Gompertz model and not to the nominal inoculation value.

Parameter A ranged from 1.76 ± 0.21 to 2.48 ± 0.30, with no statistically significant differences between treatments ($p > 0.05$). The apparent maximum growth rate (μ_{max}) showed significant differences ($p < 0.05$), with higher values observed in P-LG, S-LG, and S-US-LG, while P-US-LG showed the lowest value. The adaptation or latency phase time (λ) ranged from 2.05 ± 0.62 to 4.38 ± 1.31 h, with statistically significant differences between treatments ($p < 0.05$).

The statistically significant differences observed between treatments may be associated with variations in the structure and availability of protein substrates, resulting from both protein solubilization and ultrasound pretreatment.

Acidification Kinetics

The variation in pH during the fermentation of pea protein concentrates by *L. gasseri* is shown in Fig. 3. In all treatments, a progressive reduction in pH was observed over time, with characteristic sigmoidal behavior, adequately described by the four-parameter logistic model.

The experimental data (mean ± standard deviation; $n = 3$) showed high coefficients of determination ($R^2 = 0.951$–0.989), indicating an excellent fit of the model to the acidification profiles (Table 2).

Table 1 Kinetic parameters estimated by the modified Gompertz model (y_0, A, μ_{max}, and λ) for the four experimental treatments, including coefficients of determination (R^2) and standard deviations ($n = 5$), obtained for pea protein concentrates fermented by *L. gasseri*. Distinct lowercase superscript letters indicate statistically significant differences between means according to Tukey's test ($p < 0.05$). For the post-peak exponential fit, only R^2 values are shown because parameter estimates were not interpreted statistically due to inadequate fit in most treatments

Gompertz model				
Parameter	P-LG	P-US-LG	S-LG	S-US-LG
y_0 (Log cell/mL)	7.19 ± 0.13^{a}	6.85 ± 0.12^{ab}	6.62 ± 0.12^{ab}	6.42 ± 0.12^{b}
A (dimensional)	1.77 ± 0.21^{a}	2.48 ± 0.30^{a}	2.34 ± 0.28^{a}	1.76 ± 0.21^{a}
μ_{max} (Log/h)	0.425 ± 0.12^{a}	0.0967 ± 0.03^{b}	0.362 ± 0.10^{a}	0.497 ± 1.13^{a}
λ (h)	3.67 ± 1.10^{a}	2.05 ± 0.62^{b}	2.61 ± 0.78^{b}	4.38 ± 1.31^{a}
R^2 (adimensional)	0.91	0.86	0.95	0.97
Post-peak exponential fit (descriptive)				
R^2 (adimensional)	0.593	0.018	0.368	0.046

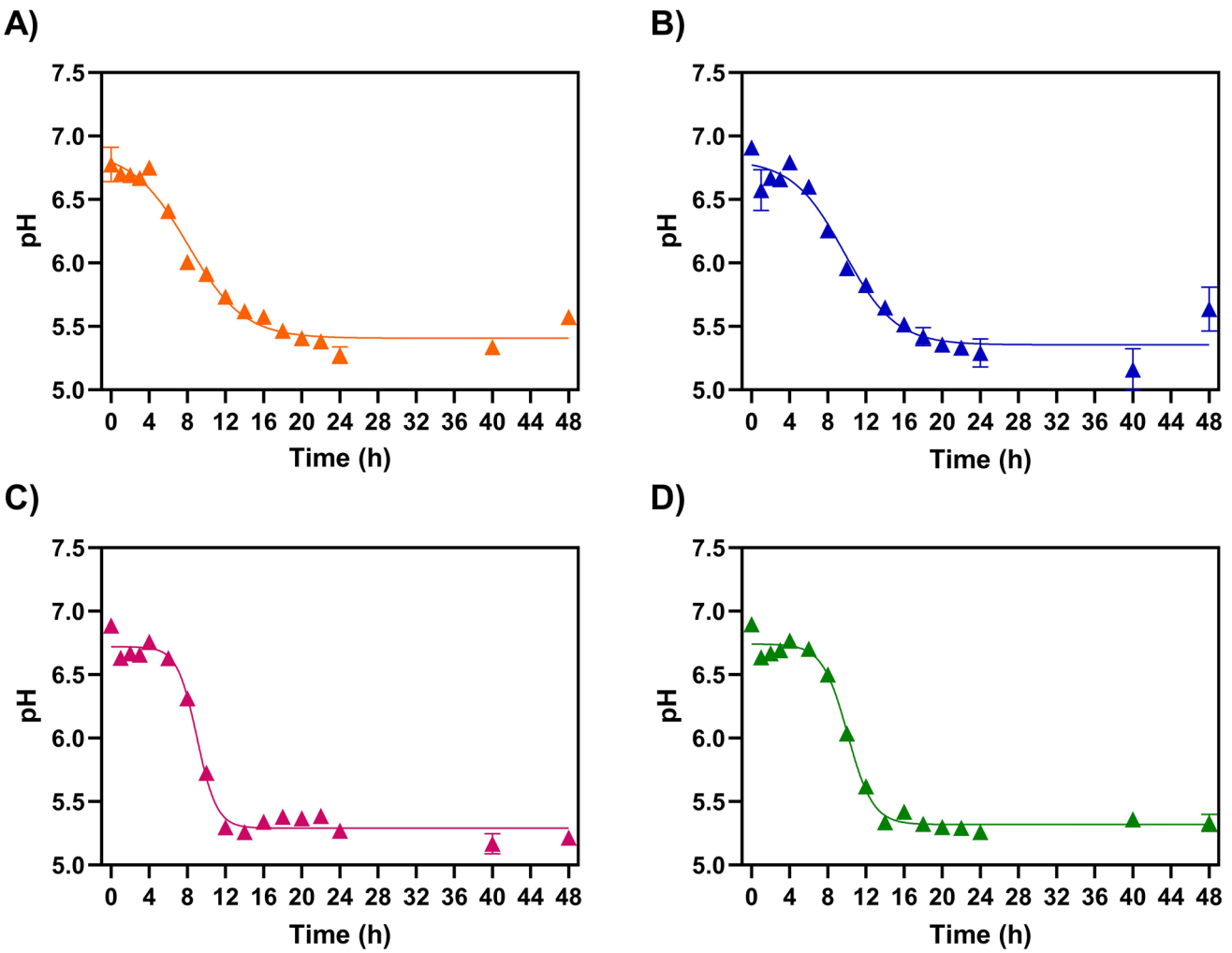


Fig. 3 Variation of pH during fermentation over time for the four experimental treatments applied to pea protein concentrates fermented by *L. gasseri*. The points represent the experimental means accompanied by the standard deviation ($n = 3$), for each treatment: **A** P-LG (protein fermented with *L. gasseri*; orange and red), **B** P-US-LG (protein pretreated with ultrasound and fermented with *L. gasseri*, blue), **C** S-LG (soluble protein fermented with *L. gasseri*; pink), and **D** S-US-LG (soluble protein pretreated with ultrasound and fermented with *L. gasseri*). The lines correspond to the fits of the four-parameter logistic model to the experimental pH data

Table 2 Kinetic parameters estimated by the four-parameter logistic model (A, B, C, D) for the four experimental treatments, including the coefficients of determination (R^2) and respective standard deviations ($n = 3$), obtained for pea protein concentrates fermented by *L. gasseri*. Distinct lowercase superscript letters indicate statistically significant differences between means according to Tukey's test ($p < 0.05$)

Four-parameter logistic model				
Parameter	P-LG	P-US-LG	S-LG	S-US-LG
A (pH)	6.883 ± 0.071^{a}	6.811 ± 0.067^{a}	6.720 ± 0.022^{a}	6.741 ± 0.018^{a}
B (ΔpH)	-1.476 ± 0.083^{a}	-1.456 ± 0.085^{a}	-1.429 ± 0.029^{a}	-1.422 ± 0.025^{a}
C (h)	8.051 ± 0.443^{c}	9.716 ± 0.487^{a}	9.012 ± 0.137^{b}	10.088 ± 0.132^{a}
D (h)	2.927 ± 0.364^{a}	2.700 ± 0.442^{a}	1.042 ± 0.115^{b}	1.327 ± 0.116^{b}
R^2 (adimensional)	0.974	0.951	0.985	0.989

The initial pH values (estimated by parameter *A*) were similar among treatments ($p > 0.05$), ranging from 6.72 ± 0.02 to 6.88 ± 0.07. The magnitude of the total pH reduction (parameter *B*) also did not differ significantly among treatments ($p > 0.05$), ranging from -1.42 ± 0.03 to -1.48 ± 0.08.

Statistically significant differences ($p < 0.05$) were observed for parameter *C*, associated with the characteristic acidification time, which ranged from 8.05 ± 0.44 h (P-LG) to 10.09 ± 0.13 h (S-US-LG). Parameter *D*, related to the slope of the curve and the rate of pH decline, showed significantly lower values in the S-LG and S-US-LG treatments compared to P-LG and P-US-LG ($p < 0.05$).

Taken together, the results show distinct acidification profiles among the treatments, with differences mainly associated with the temporal kinetics of pH reduction, while the initial values and total amplitude of acidification remain similar.

Kinetics of Total Soluble Solid Consumption

The variation in total soluble solids content (°Brix) over the fermentation time of pea protein concentrates by *L. gasseri* is shown in Fig. 4. In all treatments, a general trend of reduction in total solids was observed during the initial hours of fermentation, followed by stabilization of values throughout the evaluated period. Data are expressed as mean ± standard deviation ($n = 3$).

In the P-LG treatment (Fig. 4A), the initial values of total soluble solids were around 5.43 ± 0.802°Brix, showing a progressive decrease to 3.93 ± 0.231°Brix at the end of fermentation. The P-US-LG treatment (Fig. 4B) showed

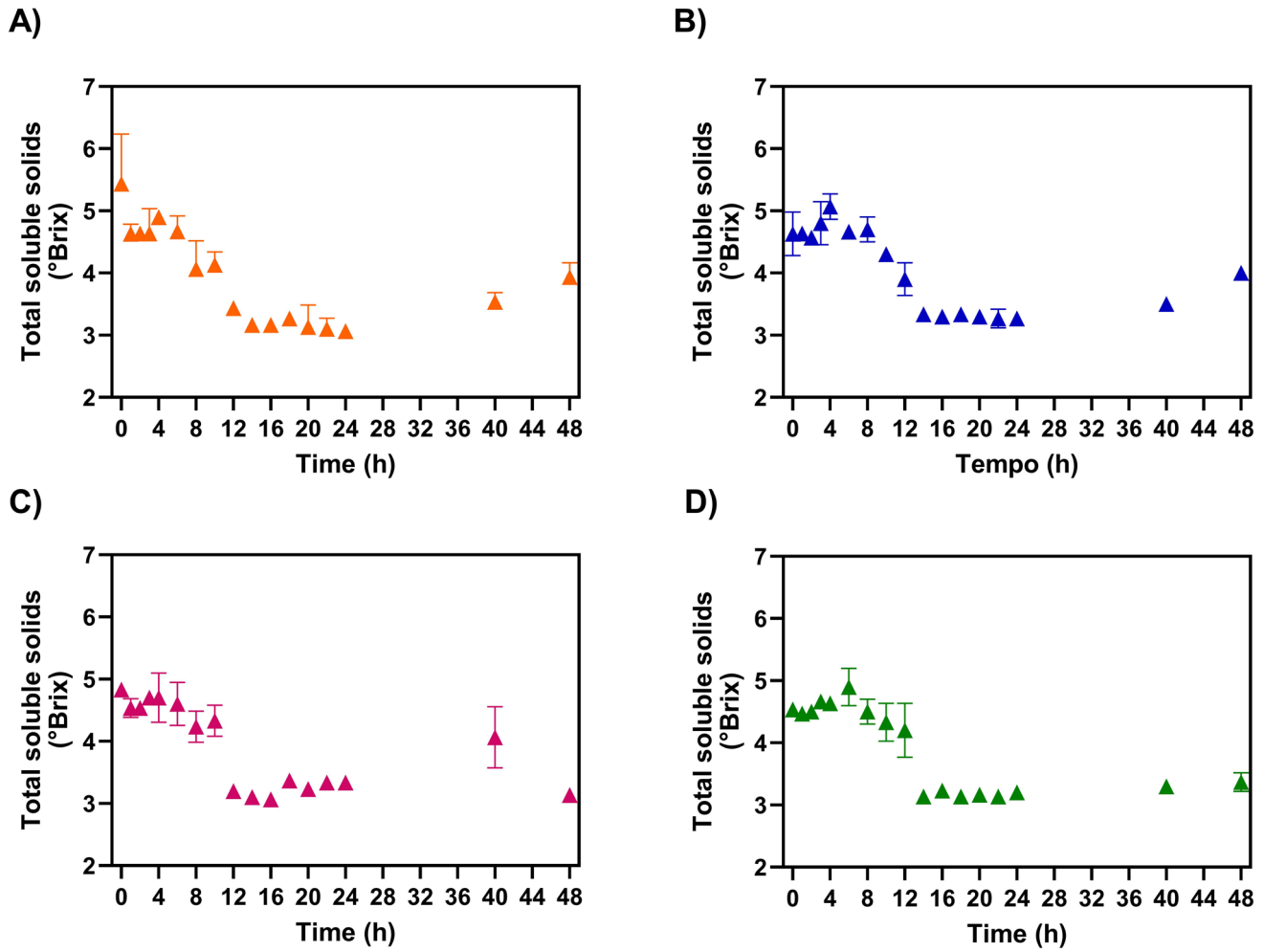


Fig. 4 Variation in total soluble solids content during fermentation over time for the four experimental treatments applied to pea protein concentrates fermented by *L. gasseri*. The points represent the experimental means accompanied by the standard deviation ($n = 3$) for each treatment: **A** P-LG (protein fermented with *L. gasseri*; orange and red), **B** P-US-LG (protein pretreated with ultrasound and fermented with *L. gasseri*, blue), **C** S-LG (soluble protein fermented with *L. gasseri*; pink), and **D** S-US-LG (soluble protein pretreated with ultrasound and fermented with *L. gasseri*)

similar behavior, with initial values of 4.63 ± 0.351°Brix, followed by a gradual reduction to 4.0 ± 0.10°Brix at the end of fermentation.

For the S-LG treatment (Fig. 4C), the initial average value was 4.83 ± 0.058°Brix, showing a progressive decrease to 3.13 ± 0.058°Brix after 48 h of fermentation. Similarly, the S-US-LG treatment (Fig. 4D) showed a progressive reduction in total soluble solids, starting from 4.53 ± 0.115°Brix and reaching an average value of 3.37 ± 0.153°Brix after 48 h of fermentation. These overall results indicate similar profiles of total soluble solids consumption among the treatments, with differences mainly associated with the initial values, suggesting interference from the ultrasound and centrifugation pretreatments in the availability of soluble solids as a substrate for *L. gasseri*.

Shear Viscosity

The rheological behavior of pea protein concentrates fermented by *L. gasseri* was presented in Fig. 5. In all treatments, the samples exhibited non-Newtonian pseudoplastic behavior, characterized by a decrease in apparent viscosity with increasing shear rate, both at the beginning of fermentation (0 h) and at the end (after 48 h), regardless of the measurement temperature (25 and 37 °C). The temperatures of 25 °C and 37 °C were chosen because they represent the average ambient temperature (25 °C) and the incubation temperature during fermentation (37 °C).

The P-LG and P-US-LG formulations (Fig. 5A–D) showed substantially higher apparent viscosity values than those observed for the soluble protein-based formulations (S-LG and S-US-LG; Fig. 5E–H), especially at low shear rates. For these systems, fermentation for 48 h resulted in a pronounced reduction in apparent viscosity throughout the entire shear range evaluated, an effect most evident in measurements taken at 37 °C. In contrast, the S-LG and S-US-LG treatments showed significantly lower viscosity values and less variation throughout the fermentation process, maintaining relatively stable rheological profiles.

The rheological parameters estimated by the Ostwald-de Waele model are presented in Table 3. The factorial ANOVA (4 × 2 × 2) showed that both the consistency index (k) and the flow behavior index (n) were significantly influenced by the treatment, temperature, and fermentation time factors ($p < 0.001$), as well as by their second- and third-order interactions ($p < 0.001$), demonstrating that the rheological response of the systems depends on the combination of these experimental variables.

For the consistency index (k), significant main effects of treatment, temperature, and time were observed, in addition to significant treatment × temperature, treatment × time, temperature × time, and treatment × temperature × time interactions. In general, the highest k values were observed in the P-LG and P-US-LG experimental conditions at the initial time (0 h), especially at 25 °C, reflecting greater resistance to flow under these conditions. Fermentation for 48 h promoted significant reductions in k, particularly in P-LG, an effect intensified at 37 °C, characterizing a response dependent on the interaction between time and temperature. In P-US-LG, the magnitude of the reduction in k was modulated by temperature, corroborating the presence of a third-order interaction. In contrast, the soluble S-LG and S-US-LG systems showed significantly lower k values under all conditions, with less pronounced variations throughout fermentation and at different temperatures, indicating lower structural sensitivity of these systems to the evaluated conditions.

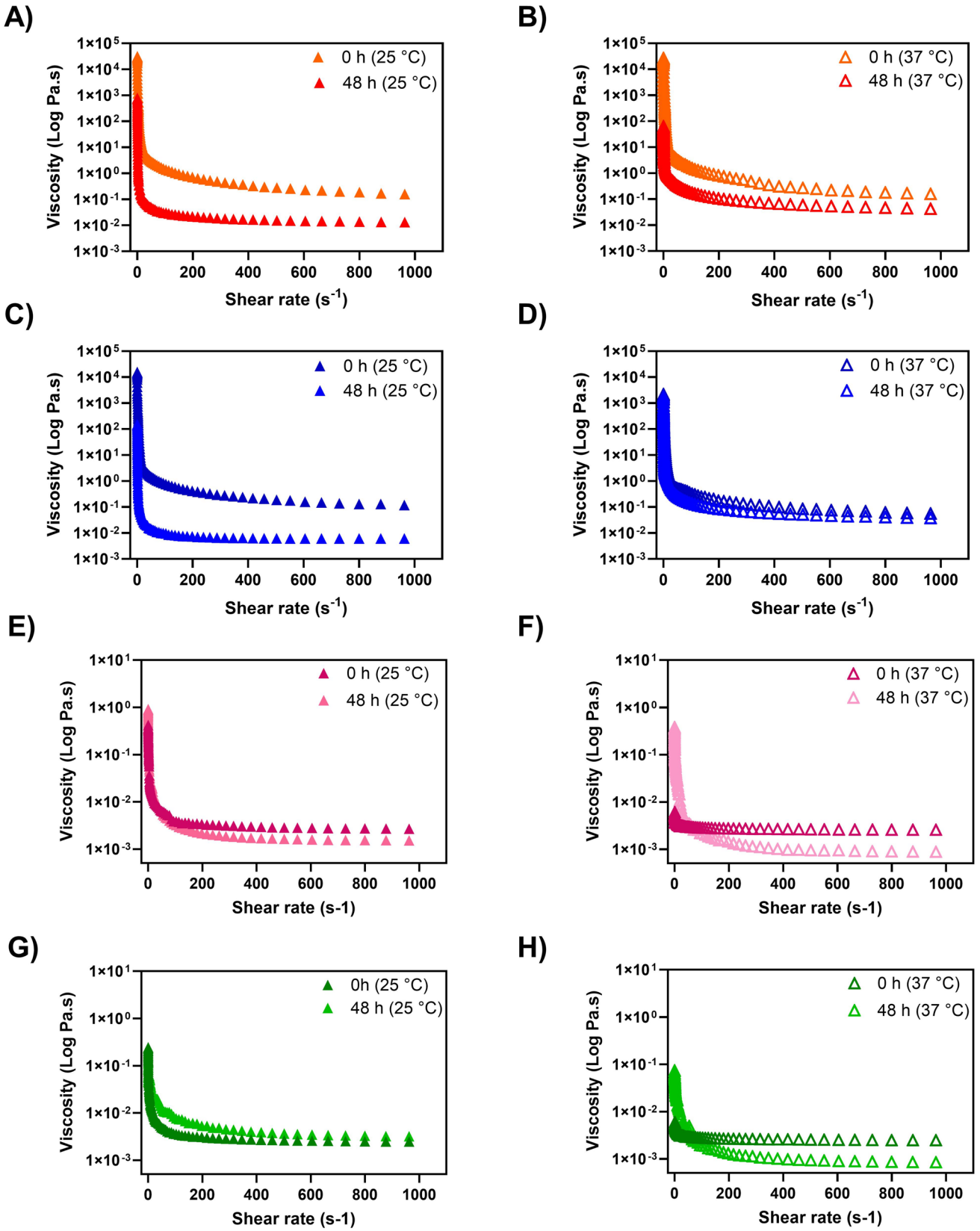
The flow behavior index (n) showed significant main effects of treatment, temperature, and time ($p < 0.001$), as well as significant second- and third-order interactions. These results indicated that, although all samples exhibit non-Newtonian behavior, the variations in n are strongly dependent on the combination of factors. In general, lower n values were observed in the integral systems (P-LG and P-US-LG), characterizing more pronounced pseudoplastic behavior, while the soluble systems (S-LG and S-US-LG) showed higher n values, especially at 37 °C, indicating a flow behavior less dependent on the shear rate. Changes in n throughout fermentation were particularly evident in the soluble systems, reflecting structural modifications induced by the process and fermentation conditions.

Taken together, the statistical results demonstrate that k is the parameter most sensitive to structural changes induced by fermentation, temperature, and pretreatments, while n responds more subtly, but is significantly dependent on the interactions between the factors. The high coefficients of determination ($R^2 = 0.928$–0.998) confirm the excellent suitability of the Ostwald-de Waele model to describe the rheological behavior of the different experimental conditions.

Oscillatory Frequency Sweep

The dynamic viscoelastic behavior of pea protein concentrates fermented by *L. gasseri* was presented in Fig. 6, expressed by the storage modulus (G′), loss modulus (G″), and complex viscosity as a function of angular frequency. In all treatments, the rheological parameters exhibited a clear frequency dependence, with a decrease in complex viscosity as frequency increased, indicating non-Newtonian behavior typical of structured systems.

The P-LG (Fig. 6A, B) and P-US-LG (Fig. 6C, D) formulations show high G′ values compared to G″ throughout the entire evaluated frequency range, both at 25 °C (filled symbols) and 37 °C (open symbols), characterizing the


A)
Viscosity (Log Pa.s)
Shear rate (s-1)
0 h (25 °C)
48 h (25 °C)
B)
0 h (37 °C)
48 h (37 °C)
C)
0 h (25 °C)
48 h (25 °C)
D)
0 h (37 °C)
48 h (37 °C)
E)
0 h (25 °C)
48 h (25 °C)
F)
0 h (37 °C)
48 h (37 °C)
G)
0h (25 °C)
48 h (25 °C)
H)
0 h (37 °C)
48 h (37 °C)

◂**Fig. 5** Rheological behavior of four experimental treatments, expressed as apparent viscosity as a function of shear rate (0.1—1000 s^{-1}) for pea protein concentrates fermented by *L. gasseri*. Each panel compares the average values of the curves obtained immediately after preparation (0 h) and after 48 h of fermentation with *L. gasseri*, measured at 25 °C (filled symbols) and 37 °C (open symbols). The formulations evaluated were as follows: **A–B** P-LG (protein fermented with *L. gasseri*; 0 h—orange, 48 h—red), **C–D** P-US-LG (protein pre-treated with ultrasound and fermented with *L. gasseri*; 0 h—blue, 48 h—dark blue), **E–F** S-LG (soluble protein fermented with *L. gasseri*; 0 h—dark pink, 48 h—light pink), and **G–H** S-US-LG (soluble protein pre-treated with ultrasound and fermented with *L. gasseri*; 0 h—dark green, 48 h—light green)

predominance of the elastic character. After 48 h of fermentation, a consistent reduction in G′, G″, and complex viscosity values was observed, particularly at low frequencies, an effect more pronounced in measurements taken at 37 °C, although the condition G′ > G″ was maintained.

In contrast, the S-LG (Fig. 6E, F) and S-US-LG (Fig. 6G, H) treatments showed substantially lower G′ and G″ values across the entire frequency range when compared to the non-centrifuged treatments. In these treatments, G″ was comparable to or higher than G′ at low frequencies, especially after 48 h of fermentation and at 37 °C, indicating viscous behavior. Complex viscosity remained low and strongly frequency-dependent, reflecting less organized structures.

Increasing the measurement temperature from 25 to 37 °C resulted in a systematic decrease in G′, G″, and complex viscosity values in all treatments, regardless of fermentation time. Overall, the results demonstrate that the type of protein fraction, ultrasound pretreatment, fermentation time, and analysis temperature significantly influenced the viscoelastic response of protein concentrates fermented by *L. gasseri*.

Integrated Profile of Fermentative and Rheological Response

To provide a concise visual comparison of the main responses across the four treatments after 48 h of fermentation at 37 °C, a radar chart was constructed using five normalized key parameters: apparent maximum growth rate (μ_{max}), pH at the end of fermentation (pH), change in total soluble solids (Δ°Brix), consistency index (k), and flow behavior index (n) (Fig. 7). Values were min–max normalized (0–1) per variable to enable relative profiling. The soluble protein treatments (S-LG and S-US-LG) displayed expanded profiles in fermentative parameters (higher μ_{max}, pH, Δ°Brix, and n), indicating enhanced microbial activity, substrate utilization, and fluid-like behavior (low k). In contrast, non-centrifuged treatments (P-LG and P-US-LG) showed prominent extension towards high *k*, reflecting greater structural consistency and lower fermentative intensity. Ultrasound pretreatment modestly modulated these profiles, with a noticeable enhancement of μ_{max} in the soluble fraction.

Discussion

The results obtained demonstrate that ultrasound pretreatment and removal of insoluble solids exert synergistic effects on the fermentation kinetics with *L. gasseri* and the rheological properties of pea protein concentrate, with potential implications for the development of functional foods based on plant-based proteins. These results demonstrate the potential of employing technologies such as ultrasound and probiotic fermentation to enhance the functionality of alternative proteins, thereby promoting greater accessibility to bioactive food formulations.

The shorter lag phase (λ) observed in P-US-LG (2.05 ± 0.62 h) compared with P-LG (3.67 ± 1.10 h) can be attributed to the synergistic effect of ultrasonic pretreatment on the non-centrifuged pea protein matrix, which still contains insoluble solids. Ultrasonic cavitation likely promoted partial disruption of protein aggregates, reduced particle size, and exposed hydrophobic and hydrophilic groups, increasing the surface area of the insoluble fraction, mainly globulins such as legumin and vicilin. These structural modifications may have improved the initial accessibility of nutrients and interaction sites for *L. gasseri*, facilitating faster metabolic adaptation and reducing the time required to initiate active growth (Jadhav et al., 2024; Rahman & Lamsal, 2021; Su & Cavaco-Paulo, 2021). In contrast, the soluble fractions (S-LG and S-US-LG) did not show a reduction in the lag phase after ultrasound treatment. After centrifugation, the matrix is already enriched in soluble proteins and peptides with relatively high bioavailability, which likely shortens the baseline adaptation time and limits additional improvements by ultrasound. Moreover, because ultrasound was applied before centrifugation, many of the structural changes induced in insoluble aggregates were removed with the sediment, reducing their potential influence on bacterial adaptation in the soluble systems. Although ultrasound pretreatment initially increased substrate complexity, all treatments maintained post-peak total cell counts above 7 Log cells/mL.

The limited adequacy of the exponential decay model in the post-peak phase is biologically plausible in this system. Direct counting in a Neubauer chamber estimates the total number of counted cells and does not distinguish viable from nonviable cells, while the pea-protein matrix may contain particles and aggregates that interfere with microscopic counting. In addition, the P-US-LG and S-US-LG curves displayed post-peak stabilization/tailing rather than a monotonic first-order decline. Thus, the post-peak phase is better interpreted as an apparent change in the total number of

Table 3 Rheological parameters (k, n) adjusted by the Ostwald–de Waele model for the four experimental treatments, accompanied by their respective standard deviations and coefficients of determination (R^2), obtained for the pea protein concentrates fermented by *L. gasseri*. The data were analyzed using a 4 × 2 × 2 factorial ANOVA (treatment × temperature × fermentation time), followed by Tukey's test. Lowercase superscript letters indicate statistically significant differences between the factor combinations ($p < 0.05$)

Experiment	Temperature (°C)	Time (h)	Parameters		
			K	***n***	R^2
P-LG	25	0	4073.64 ± 283.03^{a}	0.47 ± 0.02^{cd}	0.988
		48	76.64 ± 5.59^{d}	0.09 ± 0.03^{h}	0.973
	37	0	3359.84 ± 224.30^{b}	0.43 ± 0.02^{d}	0.990
		48	10.65 ± 0.19^{d}	0.16 ± 0.01^{hg}	0.998
P-US-LG	25	0	2060.53 ± 129.49^{d}	0.42 ± 0.02^{d}	0.988
		48	10.94 ± 0.83^{d}	0.18 ± 0.04^{fg}	0.981
	37	0	247.23 ± 11.46^{d}	0.25 ± 0.02^{ef}	0.988
		48	127.74 ± 9.63^{d}	0.17 ± 0.03^{g}	0.977
S-LG	25	0	0.151 ± 0.002^{d}	0.29 ± 0.01^{e}	0.995
		48	0.240 ± 0.003^{d}	0.28 ± 0.01^{e}	0.997
	37	0	0.005 ± 0.000^{d}	0.89 ± 0.005^{a}	0.938
		48	0.114 ± 0.001^{d}	0.32 ± 0.01^{e}	0.997
S-US-LG	25	0	0.083 ± 0.001^{d}	0.31 ± 0.01^{e}	0.996
		48	0.063 ± 0.002^{d}	0.69 ± 0.02b	0.928
	37	0	0.005 ± 0.000^{d}	0.87 ± 0.005^{a}	0.950
		48	0.045 ± 0.000^{d}	0.53 ± 0.01^{c}	0.991

counted cells than as strict death kinetics. In this context, non-log-linear survival models such as Weibull-type models, which can accommodate curvature and tailing, may be more appropriate than a simple exponential decay model (Albert & Mafart, 2005; Mafart et al., 2002).

The soluble treatments (S-LG and S-US-LG) showed the highest apparent maximum growth rate ($\mu_{max} = 0.362$–0.497 Log/h) when compared to the P-US-LG treatment (0.0097 Log/h), demonstrating that differences in the physicochemical properties of the medium and in the accessibility to nutrients, resulting from the removal of insoluble solids, exert a direct influence on the growth kinetics of *L. gasseri.* Similar results were reported by Lima et al. (2022), who demonstrated that the physicochemical characteristics and nutritional composition of the medium are determinants for the growth rate of *L. gasseri* in passion fruit juice. Additionally, considering the nutritional complexity required for the optimal growth of lactic acid bacteria, including the availability of peptides and carbohydrates, it is evident that modifications to the fermentation matrix, whether by removing insoluble solids or by ultrasound pretreatment, can significantly modulate the efficiency with which the microorganism reaches its maximum growth potential (Kwoji et al., 2022).

The reduction in pH and total soluble solids throughout fermentation is consistent with the production of lactic acid and the utilization of substrates present in pea protein concentrate, a phenomenon widely known in lactic fermentations, where the metabolism of substrates present in the medium leads to acidification of the medium and the establishment of an environment unfavorable to further microbial growth after a certain point in fermentation (Kaleda et al., 2025). This behavior also coincides with reports of lactic fermentation in other plant systems, where the drop in pH accompanies the accumulation of acidic metabolites, leading to the stabilization of the microbial population as the medium reaches inhibitory acidity levels (Lima et al., 2022; Monteiro et al., 2020).

In terms of rheological properties, the significant differences between the solubilized and soluble solids-containing treatments observed in this study include higher consistency (k) values and a predominance of elastic characteristics in P-LG and P-US-LG, in contrast to more viscous and less structured profiles in S-LG and S-US-LG. These observations can be directly linked to fermentation-induced structural changes in the protein matrix (Emkani et al., 2021). During lactic acid fermentation with *L. gasseri*, progressive acidification (pH drop to ~ 5.4–5.5) approaches the isoelectric point of pea proteins (around pH 4.5–5.5 for vicilin and legumin fractions), reducing net charge and electrostatic repulsion between protein molecules (Masiá et al., 2024). This promotes enhanced protein–protein interaction, particularly hydrophobic associations and hydrogen bonding, leading to partial aggregation and the formation of a more cohesive, elastic network as evidenced by $G' > G''$ across frequencies in non-centrifuged systems. Simultaneously, proteolytic activity of *L. gasseri* (via cell-envelope proteases and intracellular peptidases) induces limited hydrolysis of pea proteins (primarily vicilin/convicilin susceptible fractions), generating smaller peptides that disrupt overly tight aggregates while exposing hydrophobic regions (Klost et al., 2020). This dual mechanism, acidification-driven aggregation combined with moderate proteolysis, explains the observed reduction in apparent viscosity and consistency index (k) after 48 h of fermentation, particularly pronounced

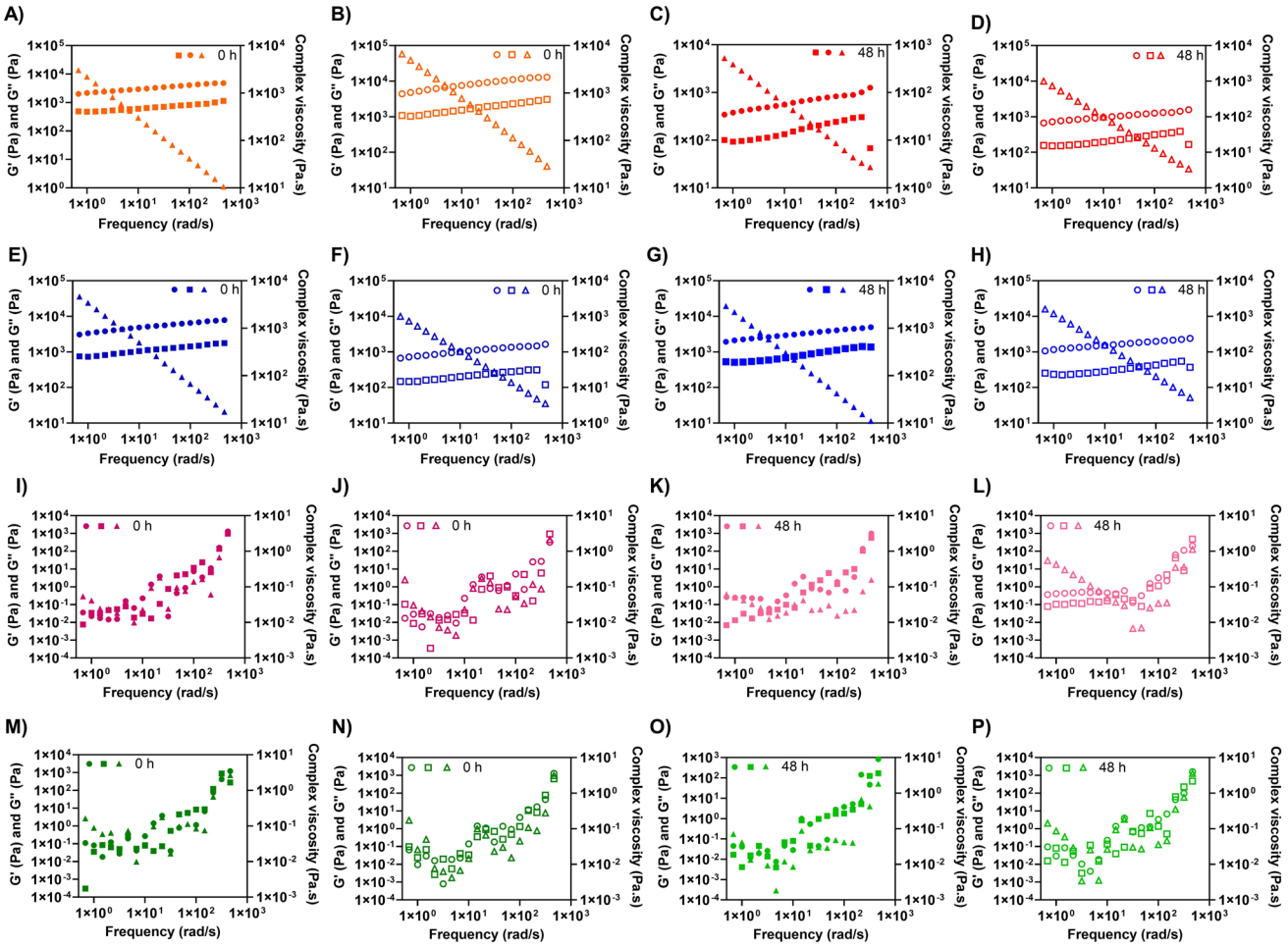


Fig. 6 Rheological behavior of four experimental treatments, expressed as storage modulus (G′, circle), loss modulus (G″, square), and complex viscosity (triangle), obtained for pea protein concentrates fermented by *L. gasseri.* Each panel compares the average values of the curves obtained immediately after preparation (0 h) and after 48 h of fermentation with *L. gasseri*, measured at 25 °C (filled symbols) and 37 °C (open symbols). The formulations evaluated were as follows: **A–D** P-LG (protein fermented with *L. gasseri*; 0 h—orange, 48 h—red), **E–H** P-US-LG (protein pre-treated with ultrasound and fermented with *L. gasseri*; 0 h—blue, 48 h—dark blue), **I–L** S-LG (soluble protein fermented with *L. gasseri*; 0 h—dark pink, 48 h—light pink) and **M–P** S-US-LG (soluble protein pre-treated with ultrasound and fermented with *L. gasseri*; 0 h—dark green, 48 h—light green)

at 37 °C, where thermal energy further facilitates partial unfolding and reorganization of protein networks without full denaturation. This is consistent with the literature showing that lactic fermentation can modify protein–protein and protein-water interactions, directly impacting the structural network and responses to shear stress (Masiá et al., 2024). In protein matrices, acidification and microbial enzymatic activity can lead to partial denaturation and reorganization of protein aggregates, affecting the ability to form stable three-dimensional networks, as described for fermented pea and lentil protein systems (Masiá et al., 2022; Tonini et al., 2024).

The predominance of G′ over G″ in the P-LG and P-US-LG treatments suggests the formation of a more cohesive and structured network, possibly associated with a greater presence of intact protein fractions and physicochemical interactions favoring elastic resistance, with post-fermentation reductions (Silva et al., 2025). In contrast, soluble formulations lack these aggregates, favoring viscous flow due to their limited binding capacity after centrifugation.

Furthermore, the significant effects of measurement temperature (25 °C vs. 37 °C) and fermentation time on rheological parameters reflect underlying mechanisms related to thermal energy promoting partial protein unfolding, exposure of hydrophobic domains, and enhanced molecular mobility, facilitating aggregation or reorganization after fermentation. This results in lower G′, G″, and complex viscosity, as well as sharper reductions in consistency index (k), especially in non-centrifuged systems. In contrast, at 25 °C, reduced thermal agitation preserves more rigid

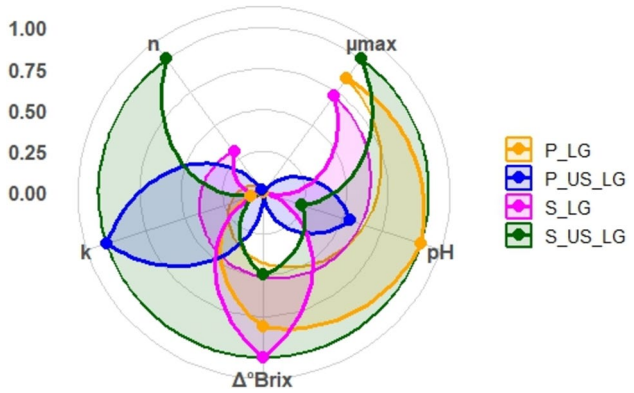


Fig. 7 Radar chart illustrating the comparative profiles of key fermentative and rheological parameters (μ_{max}, pH, Δ°Brix, k, and n) across the four experimental treatments after 48 h of fermentation at 37 °C. Values are min–max normalized (0–1) per variable for relative comparison

structures, yielding higher viscoelastic moduli and consistency. These temperature-dependent shifts align with known pea protein behavior, where moderate heating (below full denaturation ~ 90 °C) induces limited unfolding and aggregation via hydrophobic interactions without extensive covalent crosslinking, modulating viscoelastic response in fermented matrices (Kuang et al., 2023; Langendörfer et al., 2024).

The radar chart (Fig. 7) provides a clear visual integration of the responses, confirming that the presence/absence of insoluble solids is the dominant factor differentiating the profiles (higher fermentative activity and fluidity in soluble fractions vs. greater consistency in non-centrifuged systems), while ultrasound acts as a secondary modulator, particularly enhancing μ_{max} in soluble matrices.

These findings have relevant implications for food applications, particularly in the development of plant-protein-based fermented products, where lactic fermentation can be used not only to improve nutritional and sensory quality but also to modulate technological properties such as texture and rheological stability. The structural behavior of these systems is strongly influenced by the composition of pea protein concentrates, whose insoluble fraction is mainly composed of poorly soluble globulin aggregates, especially legumin and vicilin, which play a key role in determining the structural and functional properties of the protein matrix (Tahir et al., 2024). These proteins participate in the formation of gel networks stabilized primarily by hydrophobic and electrostatic interactions, thereby influencing the rheological characteristics of fermented systems (Klost et al., 2020). During lactic fermentation, microbial proteolytic activity can modify the polypeptide profile and increase protein solubility by generating smaller peptides (Emkani et al., 2021; Kim et al., 2024), thereby enhancing substrate accessibility and metabolic utilization by lactic acid bacteria. This mechanism may explain the improved fermentation performance observed in soluble systems. In addition, processing and protein isolation steps can promote aggregation of pea globulins, affecting the structural organization of the protein network and its macroscopic properties (Luecha et al., 2024). However, it should be noted that the present study was conducted under controlled conditions and with a limited number of matrices and operational parameters, which may limit the direct extrapolation of the results to more complex food systems or pilot-scale processes. Nevertheless, the findings suggest that integrated formulation and processing strategies, including solids separation in protein concentrates and physical pretreatments, can be adjusted to optimize microbial performance and final physicochemical properties, thereby expanding the potential application of fermented pea protein concentrates in innovative food systems.

Conclusion

The removal of insoluble solids was the main determining factor in the fermentative and rheological responses of pea protein matrices fermented by *L. gasseri*, resulting in less structured systems with lower consistency index (k) values and higher flow behavior index (n) values. Ultrasound pretreatment modulated these responses in a manner dependent on the protein fraction, the temperature analyzed, and the fermentation process, as evidenced by the significant interactions observed in the factorial ANOVA. Multivariate analyses corroborated these findings, indicating that the composition of the protein matrix governed the overall organization of the kinetic, acidification, and rheological variables, while ultrasound acted as a secondary modulator, highlighting the potential of combined fractionation and ultrasonic pretreatment strategies for adjusting the technological properties of fermented plant systems. The substantial reduction in consistency (k) and the shift to higher n values after fermentation, particularly pronounced in noncentrifuged matrices at 37 °C, result in systems with improved flow behavior and reduced structural stiffness, expanding their potential for incorporation into innovative food formulations. These adjusted properties are especially suitable for high-protein fermented beverages (e.g., plant-based fermented beverages with improved flowability, sedimentation stability, and a smoother mouthfeel), viscous or semi-fluid products (e.g., creams, sauces, or fermented pastes with adjustable consistency and reduced bean flavor), and as functional ingredients in gel or emulsified matrices where moderate viscosity and controlled viscoelasticity are desired without excessive firmness. In practical food processing contexts, the observed rheological adjustment, facilitated by acidification close to the isoelectric point combined with limited proteolysis, allows for clean-label texture modulation, improved industrial-scale

processability, and the development of sustainable, lactose-free, high-protein alternatives with enhanced sensory and functional performance. Future studies will include detailed physicochemical characterization of the substrates under the most effective conditions identified here to confirm the mechanistic links between pretreatment, substrate accessibility, and fermentation performance.

Author Contribution Antônia Isabelly Monteiro dos Anjos: Conceptualization, Data curation, Investigation, Methodology, Writing – original draft. Shênia Santos Monteiro: Methodology, Formal analysis, Visualization, Writing – review and editing. Anna Clara Batista de Sousa: Investigation, Methodology. Marcus Vinícius Lia Fook: Resources, Methodology. Daniel Pens Gelain: Supervision, Writing – review and editing. José Cláudio Fonseca Moreira: Supervision, Writing – review and editing. Hugo Miguel Lisboa: Visualization, Formal analysis. Matheus Augusto de Bittencourt Pasquali: Conceptualization, Supervision, Resources, Funding acquisition.

Funding The Article Processing Charge (APC) for the publication of this research was funded by the Coordenação de Aperfeiçoamento de Pessoal de Nível Superior - Brasil (CAPES) (ROR identifier: 00x0ma614). This research was funded by CNPq (process nos. 408662/2024—7, 443333/2025—4, and 306165/2023—6), FINEP 01.24.0620.00 (0329/24), and FAPESQ (process nos. 47594.673.35297.10082021 and 391/2024).

Data Availability The data will be available upon request.

Declarations

Conflict of interest The authors declare no competing interests.

Open Access This article is licensed under a Creative Commons Attribution 4.0 International License, which permits use, sharing, adaptation, distribution and reproduction in any medium or format, as long as you give appropriate credit to the original author(s) and the source, provide a link to the Creative Commons licence, and indicate if changes were made. The images or other third party material in this article are included in the article's Creative Commons licence, unless indicated otherwise in a credit line to the material. If material is not included in the article's Creative Commons licence and your intended use is not permitted by statutory regulation or exceeds the permitted use, you will need to obtain permission directly from the copyright holder. To view a copy of this licence, visit http://creativecommons.org/licenses/by/4.0/.

References

Akpabli-Tsigbe, N. D. K., Osabutey, J., Mintah, B. K., Tano-Debrah, K., & Ma, Y. (2023). Cleavage of macromolecule (protein/polysaccharide)-phenolic bond in soybean cell wall through *Lactobacillus casei* and *Lactobacillus helviticus* mixed culture solid-state fermentation for chlorogenic acid extraction. *Food Bioscience, 55*, Article 102903. https://doi.org/10.1016/j.fbio.2023.102903

Albert, I., & Mafart, P. (2005). A modified Weibull model for bacterial inactivation. *International Journal of Food Microbiology, 100*(1–3), 197–211. https://doi.org/10.1016/j.ijfoodmicro.2004.10.016

Alrosan, M., Maghaydah, S., Assaf, T., Obeidat, H. J., Bawadi, H., Alu'datt, M. H., et al. (2026). Ultrasound technique: Structure-function relationship of plant-based proteins and digestibility in food applications. *European Food Research and Technology, 252*(3), Article 128. https://doi.org/10.1007/s00217-026-05061-4

Barac, M., Cabrilo, S., Stanojevic, S., Pesic, M., Pavlicevic, M., Zlatkovic, B., & Jankovic, M. (2012). Functional properties of protein hydrolysates from pea (*Pisum sativum*, L) seeds. *International Journal of Food Science & Technology, 47*(7), 1457–1467. https://doi.org/10.1111/j.1365-2621.2012.02993.x

Chen, X., Yi, J., Wen, Z., & Fan, Y. (2024). Ultrasonic pretreatment and epigallocatechin gallate incorporation enhance the formation, apparent viscosity, and antioxidant activity of pea protein amyloid-like fibrils. *Food Hydrocolloids, 149*, Article 109630. https://doi.org/10.1016/j.foodhyd.2023.109630

Emkani, M., Oliete, B., & Saurel, R. (2021). Pea protein extraction assisted by lactic fermentation: Impact on protein profile and thermal properties. *Foods (Basel, Switzerland)*. https://doi.org/10.3390/foods10030549

Erem, E., & Kilic-Akyilmaz, M. (2024). The role of fermentation with lactic acid bacteria in quality and health effects of plant-based dairy analogues. *Comprehensive Reviews in Food Science and Food Safety*. https://doi.org/10.1111/1541-4337.13402

Farshi, P., Mirmohammadali, S. N., Rajpurohit, B., Smith, J. S., & Li, Y. (2024). Pea protein and starch: Functional properties and applications in edible films. *Journal of Agriculture and Food Research, 15*, Article 100927. https://doi.org/10.1016/j.jafr.2023.100927

Jadhav, H. B., Das, M., Das, A., V, G., Choudhary, P., Annapure, U., & Alaskar, K. (2024). Enhancing the functionality of plant-based proteins with the application of ultrasound–A review. *Measurement: Food, 13*, Article 100139. https://doi.org/10.1016/j.meafoo.2024.100139

Kaleda, A., Sharma, N., Jakobson, K., Stulova, I., & Rosenvald, S. (2025). Fermentation by lactic acid bacteria during pea protein isolation reduces undesirable flavors and changes techno-functional properties. *Food Chemistry, 492*, Article 145380. https://doi.org/10.1016/j.foodchem.2025.145380

Kim, H. D., Lee, K. S., Lee, K. E., Suh, H. J., & Kim, B.-Y. (2024). Improved digestibility and bioavailability of pea protein following enzymatic treatment and fermentation by lactic acid bacteria. *Food Science and Biotechnology, 33*(3), 607–615. https://doi.org/10.1007/s10068-023-01335-9

Klost, M., Giménez-Ribes, G., & Drusch, S. (2020). Enzymatic hydrolysis of pea protein: Interactions and protein fractions involved in fermentation induced gels and their influence on rheological properties. *Food Hydrocolloids, 105*, Article 105793. https://doi.org/10.1016/j.foodhyd.2020.105793

Kuang, J., Hamon, P., Lechevalier, V., & Saurel, R. (2023). Thermal behavior of pea and egg white protein mixtures. *Foods (Basel, Switzerland)*. https://doi.org/10.3390/foods12132528

Kwoji, I. D., Okpeku, M., Adeleke, M. A., & Aiyegoro, O. A. (2022). Formulation of chemically defined media and growth evaluation of *Ligilactobacillus salivarius* ZJ614 and *Limosilactobacillus reuteri* ZJ625. *Frontiers in Microbiology*. https://doi.org/10.3389/fmicb.2022.865493

Langendörfer, L. J., Guseva, E., Bauermann, P., Schubert, A., Hensel, O., & Diakité, M. (2024). The viscoelastic behavior of legume protein emulsion gels-The effect of heating temperature and oil content on viscoelasticity, the degree of networking, and the microstructure. *Foods (Basel, Switzerland)*. https://doi.org/10.3390/foods13233875

Lima, W. D. L., Monteiro, S. S., & de B. Pasquali, M. A. (2022). Study of fermentation strategies by *Lactobacillus gasseri* for the production of probiotic food using passion fruit juice combined with green tea as raw material. *Foods (Basel, Switzerland)*. https://doi.org/10.3390/foods11101471

Liu, Y., Li, X., Liu, J., Wei, L., Liu, Y., Lu, F., et al. (2022). Focusing on Hofmeister series: Composition, structure and functional properties of pea protein extracted with food-related anions. *Food Hydrocolloids, 133*, Article 107976. https://doi.org/10.1016/j.foodhyd.2022.107976

Lu, Z. X., He, J. F., Zhang, Y. C., & Bing, D. J. (2020). Composition, physicochemical properties of pea protein and its application in functional foods. *Critical Reviews in Food Science and Nutrition, 60*(15), 2593–2605. https://doi.org/10.1080/10408398.2019.1651248

Luecha, J., Saalbrink, J., Bonilla, J. C., & Sozer, N. (2024). Process-induced protein aggregates influenced pea globulins' structure formation upon heating. *Food Structure, 42*, Article 100398. https://doi.org/10.1016/j.foostr.2024.100398

Mafart, P., Couvert, O., Gaillard, S., & Leguerinel, I. (2002). On calculating sterility in thermal preservation methods: Application of the Weibull frequency distribution model. *International Journal of Food Microbiology, 72*(1–2), 107–113. https://doi.org/10.1016/S0168-1605(01)00624-9

Masiá, C., Jensen, P. E., Petersen, I. L., & Buldo, P. (2022). Design of a functional pea protein matrix for fermented plant-based cheese. *Foods (Basel, Switzerland)*. https://doi.org/10.3390/foods11020178

Masiá, C., Ong, L., Logan, A., Stockmann, R., Gambetta, J., Jensen, P. E., et al. (2024). Enhancing the textural and rheological properties of fermentation-induced pea protein emulsion gels with transglutaminase. *Soft Matter, 20*(1), 133–143. https://doi.org/10.1039/D3SM01001E

Monteiro, S. S., Beserra, Y. A. S., Oliveira, H. M. L., & de B. Pasquali, M. A. (2020). Production of probiotic passion fruit (*Passiflora edulis* Sims f. flavicarpa Deg.) drink using *Lactobacillus reuteri* and microencapsulation via spray drying. *Foods (Basel, Switzerland), 9*(3), Article 335. https://doi.org/10.3390/foods9030335

Patil, N. D., Kumar, A., Bains, A., Fareed, M., Dhull, S. B., Nagraik, R., & Chawla, P. (2025). A review on sustainable non-thermal approaches for pea protein: Pre-treatment, extraction, modification, and applications. *Food Chemistry: X, 29*, Article 102608. https://doi.org/10.1016/j.fochx.2025.102608

Rahman, M. M., & Lamsal, B. P. (2021). Ultrasound-assisted extraction and modification of plant-based proteins: Impact on physicochemical, functional, and nutritional properties. *Comprehensive Reviews in Food Science and Food Safety, 20*(2), 1457–1480. https://doi.org/10.1111/1541-4337.12709

Shen, Y., Hong, S., Singh, G., Koppel, K., & Li, Y. (2022). Improving functional properties of pea protein through "green" modifications using enzymes and polysaccharides. *Food Chemistry, 385*, Article 132687. https://doi.org/10.1016/j.foodchem.2022.132687

Silva, R. R., Odelli, D., Descamps, A., Scudeller, L. A., Doumert, B., Perez, J., et al. (2025). Multi-scale organization and rheology of casein and pea protein mixed hydrogels formed by acidification: Effects of ratio and temperature. *Food Research International, 209*, Article 116242. https://doi.org/10.1016/j.foodres.2025.116242

Su, J., & Cavaco-Paulo, A. (2021). Effect of ultrasound on protein functionality. *Ultrasonics Sonochemistry, 76*, Article 105653. https://doi.org/10.1016/j.ultsonch.2021.105653

Tahir, A. B., Jiang, B., & Ali, K. (2024). Unraveling distinct potential of pea (*Pisum sativum* L.) fractions (legumin, vicilin and albumin) by structural and functional characterization. *Food Research International, 198*, Article 115332. https://doi.org/10.1016/j.foodres.2024.115332

Taylor, S. L., Marsh, J. T., Koppelman, S. J., Kabourek, J. L., Johnson, P. E., & Baumert, J. L. (2021). A perspective on pea allergy and pea allergens. *Trends in Food Science & Technology, 116*, 186–198. https://doi.org/10.1016/j.tifs.2021.07.017

Tonini, S., Tlais, A. Z. A., Galli, B. D., Helal, A., Tagliazucchi, D., Filannino, P., et al. (2024). Lentils protein isolate as a fermenting substrate for the production of bioactive peptides by lactic acid bacteria and neglected yeast species. *Microbial Biotechnology, 17*(1), Article e14387. https://doi.org/10.1111/1751-7915.14387

Xu, T., Sun, X., Yan, Q., Li, Z., Cai, W., Ding, J., et al. (2023). Characterization of the physiochemical properties, microstructure, and molecular interactions of a novel rice-pea protein gel. *Food Chemistry, 424*, Article 136360. https://doi.org/10.1016/j.foodchem.2023.136360

Zhang, X., Ji, G., Zhao, Y., Chen, B., Li, W., Guo, Z., et al. (2025). The fermentation mechanism of pea protein yogurt and its bean odour removal method. *Foods*. https://doi.org/10.3390/foods14193363

Publisher's Note Springer Nature remains neutral with regard to jurisdictional claims in published maps and institutional affiliations.